Proc. Natl. Acad. Sci. USA
Vol. 90, pp. 2127–2131, March 1993
Biochemistry

Charge-reversion mutagenesis of *Dictyostelium* actin to map the surface recognized by myosin during ATP-driven sliding motion

(site-directed mutagenesis/*in vitro* motility assay/force generation/actin-activated myosin ATPase)

MASAAKI JOHARA*, YOKO YANO TOYOSHIMA†, AKIHIKO ISHIJIMA‡, HIROAKI KOJIMA‡, TOSHIO YANAGIDA‡, AND KAZUO SUTOH*

*Department of Pure and Applied Sciences, College of Arts and Sciences, University of Tokyo, Komaba, Tokyo 153, Japan; †Department of Biology, Faculty of Science, Ochanomizu University, Otsuka, Tokyo 112, Japan; and ‡Department of Biophysical Engineering and Science, Osaka University, Toyonaka, Osaka 560, Japan

Communicated by Christian B. Anfinsen,§ December 14, 1992 (received for review July 29, 1992)

ABSTRACT **Amino acid residues D24/D25, E99/E100, E360/E361, and D363/E364 in subdomain 1 of *Dictyostelium* actin were replaced with histidine residues by site-directed mutagenesis. Mutant actins were expressed in *Dictyostelium* cells and purified to homogeneity. The sliding movement of mutant actin filaments on heavy meromyosin attached to a glass surface was measured to assess the effect of the mutation on the motility of actin. For two C-terminal mutants, force generated by a single actin filament and myosin was also measured. These measurements indicated that both D24/D25 and E99/E100 are involved in ATP-driven sliding, whereas E360/E361/D363/E364 are not essential for ATP-driven sliding and force generation.**

Comparison of the atomic model of filamentous (F) actin (1, 2) with a cryoelectron microscopic image of an actin–myosin complex formed in the absence of MgATP (3) showed that the actin N terminus, the loop of residues 20–25, and the hydrophobic helix of residues 340–350 are in the major contact site of the myosin head (4). The helix of residues 79–93 and the following loop are also in contact with a long extension of the myosin head (4). The helix containing acidic residues E360/E361/D363/E364 is in contact with the N-terminal segment of the alkaline light chain 1 of the myosin head (3, 5). The actin–myosin interface thus identified coincides with that identified by antibody mapping and chemical cross-linking studies (5–11).

The question is, however, whether the interface identified in the absence of MgATP is actually recognized by myosin heads during ATP-driven sliding and force generation. One approach to answer this question is to use recombinant actin (12–15). It has been shown (12) that mutational disruption of the N-terminal acidic residue cluster of *Dictyostelium* actin affected its sliding on heavy meromyosin (HMM). The result indicates that the N-terminal acidic residues are recognized by the myosin head during sliding and, possibly, force generation.

Besides the N-terminal cluster of acidic amino acid residues, several acidic residue pairs (D24/D25, E99/E100, E360/E361, and D363/E364) are found in the putative actin–myosin interface (Fig. 1). To map the actin surface recognized by the myosin head during actin–myosin sliding and force generation, these pairs of acidic residues were replaced with histidine by recombinant DNA techniques. Since it has been well-established that the ionic interaction between actin and myosin is dominant during sliding and force generation, a charge-reversion mutation at the actin–myosin interface would result in the loss of sliding and force generation. In fact, examination of the sliding of these mutant actin filaments by an *in vitro* motility assay (16, 17) showed that mutations at D24/D25 and at E99/E100 resulted in the complete or partial loss of filament sliding, indicating that they are involved in ATP-driven sliding and, possibly, force generation. A charge-reversion mutation at the C-terminal acidic-residue cluster, however, did not significantly affect sliding and force generation, indicating that this cluster is not essential for these processes.

MATERIALS AND METHODS

Plasmids. Site-directed mutagenesis was carried out according to Kunkel (18). Transformation vectors were constructed by inserting the wild-type or mutant actin 15 gene (19) into an integration vector B10Tp2′ (20) as described by Sambrook *et al.* (21).

Transformation of *Dictyostelium* Cells. Transformation vectors were introduced into *Dictyostelium* cells by the calcium phosphate method (22) or by electroporation (23). Transformed cells were selected by culturing them in the presence of G418 as described (12). Cells were cloned twice by picking them from a colony visible on a culture dish and plating them on a new dish. The expression level of mutant actin in these cloned cells was estimated by the two-dimensional gel electrophoresis (24) since all types of mutations described in this paper altered the isoelectric point of actin.

Assays. Transformed *Dictyostelium* cells were used to purify both mutant and wild-type actins to homogeneity as described (12). Wild-type actin thus prepared was used as the control in various assays on mutant actins. HMM was prepared from rabbit skeletal myosin (25).

In vitro motility assays were carried out by using rabbit skeletal HMM attached to nitrocellulose-coated glass (12, 26). Assay conditions were as follows: temperature, 25°C; HMM concentration, 50 μg/ml. The assay solvent contained 25 mM KCl, 25 mM imidazole (pH 7.4), 4 mM $MgCl_2$, 1 mM dithiothreitol, and 1 mM ATP plus the deoxygenation system (27). E99H/E100H mutant filaments have tendency to form bundles at higher concentrations. To avoid bundling of filaments, actin concentration was kept low (<0.2 mg/ml). Under these conditions, a majority of filaments were single filaments, as judged from their fluorescence intensities and unidirectional motion. Such precaution was not necessary for other mutant and wild-type actins.

The force generated by a single actin filament and full-length rabbit skeletal myosin was measured on silicon-coated glass surfaces as described (28, 29). The assay temperature was 26°C. The assay solvent contained 25 mM KCl, 20 mM Hepes (pH 7.8), 5 mM $MgCl_2$, and 2 mM ATP plus the deoxygenation system.

The publication costs of this article were defrayed in part by page charge payment. This article must therefore be hereby marked "*advertisement*" in accordance with 18 U.S.C. §1734 solely to indicate this fact.

Abbreviations: HMM, heavy meromyosin; F-actin, filamentous actin.

§Communication of this paper was initiated by William F. Harrington and, after his death (October 31, 1992), completed by Christian B. Anfinsen.

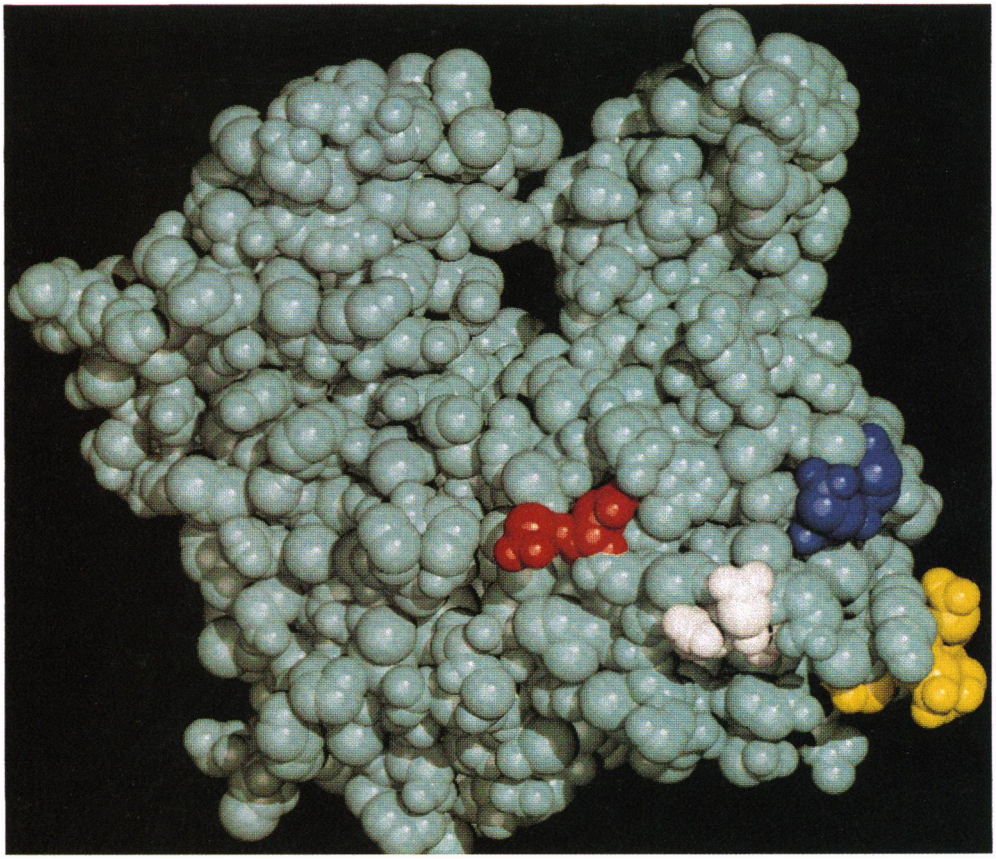

FIG. 1. Atomic model of actin showing residues replaced with histidine residues. The structure was generated by using atomic coordinates supplied by Kenneth Holmes (Max-Planck-Institute, Germany). Residues are identified as follows: white, D1/E3/D4; red, D24/D25; blue, E99/E100; yellow, E360/E361/D363/E364. Orientation of the molecule is the same as that in the original ribbon model (1).

Actin-activated ATPase activities were measured by the malachite green method (30) as described (12). The assay temperature was 25°C. The assay solvent contained 2.5 mM KCl, 10 mM Mops (pH 7.0), 4 mM $MgCl_2$, and 0.1 mM dithiothreitol. ATPase reactions were started by addition of 1 mM ATP. Filaments of wild-type actin, D24H/D25H, E360H/E361H, and D363H/E364H used in the assay were prepared as follows. Actin filaments were stabilized by phalloidin (10 μg/ml). Stabilized filaments were centrifuged and then pellets were suspended into the assay solvent to remove any free phosphate released from ATP during the polymerization of actin. Filaments were centrifuged and pellets were suspended again. Phosphate-free filaments were finally suspended in the assay solvent. These steps were necessary to obtain reliable data by the sensitive malachite green method.

RESULTS

Behavior of Mutant Actins. D24H/D25H (replacement of both D24 and D25 with histidine residues), E360H/E361H, and D363H/E364H actins formed filaments as wild-type actin. These mutant filaments bound rhodamine-phalloidin. The length distribution of fluorescent mutant filaments was very similar to that of wild-type filaments when examined under a fluorescence microscope. E99H/E100H behaved like other mutant actins except that it had tendency to form bundles at higher concentrations. A similar tendency was reported for an N-terminal mutant produced in yeast cells (14).

All types of mutant filaments tightly bound to HMM attached to a glass surface, indicating that all actins formed a rigor complex with myosin heads. Upon the addition of MgATP, motile mutants started sliding, whereas the nonmotile mutants showed Brownian motion, indicating that the rigor binding was weakened in the presence of MgATP. Thus, all types of mutants investigated here, either motile or nonmotile, formed ATP-sensitive rigor complex with myosin.

Measurements of the Sliding Velocity of Actin Filaments. *In vitro* motility assays were carried out to assess the effects of the mutations on the myosin-driven sliding velocity of actin filaments. In the absence of MgATP, rhodamine-phalloidin-labeled D24H/D25H filaments firmly bound to HMM on a nitrocellulose-coated glass surface. Upon addition of MgATP, these filaments were gradually lost from the surface by Brownian motion without sliding. This result indicates that D24H/D25H filaments had lost motility even though they formed an ATP-sensitive rigor complex with myosin.

E99H/E100H filaments had a tendency to form nonmotile bundles at higher concentrations. Velocity measurements were carried out on single filaments, which were the majority population when filaments were formed at a low concentration of actin (<0.2 mg/ml). These single filaments showed a partial loss of motility. Upon addition of MgATP, filaments slid slowly, then stopped, and resumed the slow sliding motion after a while. On average, 50% of filaments slid at a given moment at 25°C. When the temperature was increased to 30°C, >80% of filaments slid. This behavior was similar to that of the D1H/D4H mutant (12). Histograms of the velocity distribution for moving E99H/E100H filaments at 25°C are shown in Fig. 2. The average velocity was 0.8 ± 0.2 μm/sec (n = 25). Since the sliding velocity is rather sensitive to the conditions of the glass surface, wild-type actin was always prepared from the same transformed *Dictyostelium* cells to measure the velocity on the same batch of nitrocellulose-

coated glass surface. The average velocity of this control actin was 4.8 ± 0.9 μm/sec (n = 44).

Virtually all E360H/E361H filaments and all D363H/E364H filaments smoothly slid on HMM upon the addition of MgATP. The average velocity of E360H/E361H filaments was 6.0 ± 0.4 μm/sec (n = 50). The control wild-type actin slid at an average velocity of 4.6 ± 0.6 μm/sec (n = 49). The average velocity of D363H/E364H filaments was 5.2 ± 0.8 μm/sec (n = 43). The average velocity of the control actin was 4.3 ± 0.6 μm/sec (n = 41). Thus, E360H/E361H and D363H/E364H filaments slid on HMM-coated glass slightly faster than the control wild-type actin (Table 1). When driven by full-length myosin on a silicon-coated glass surface, however, the sliding velocity of these mutant actin filaments was slightly reduced. Although no explanation for this apparent discrepancy is available, we recognize that surface conditions are critical factors for the myosin (or HMM)-driven sliding of actin filaments. These data led us to conclude, at least, that mutations at E360/E361 and at D363/E364 affected sliding very slightly.

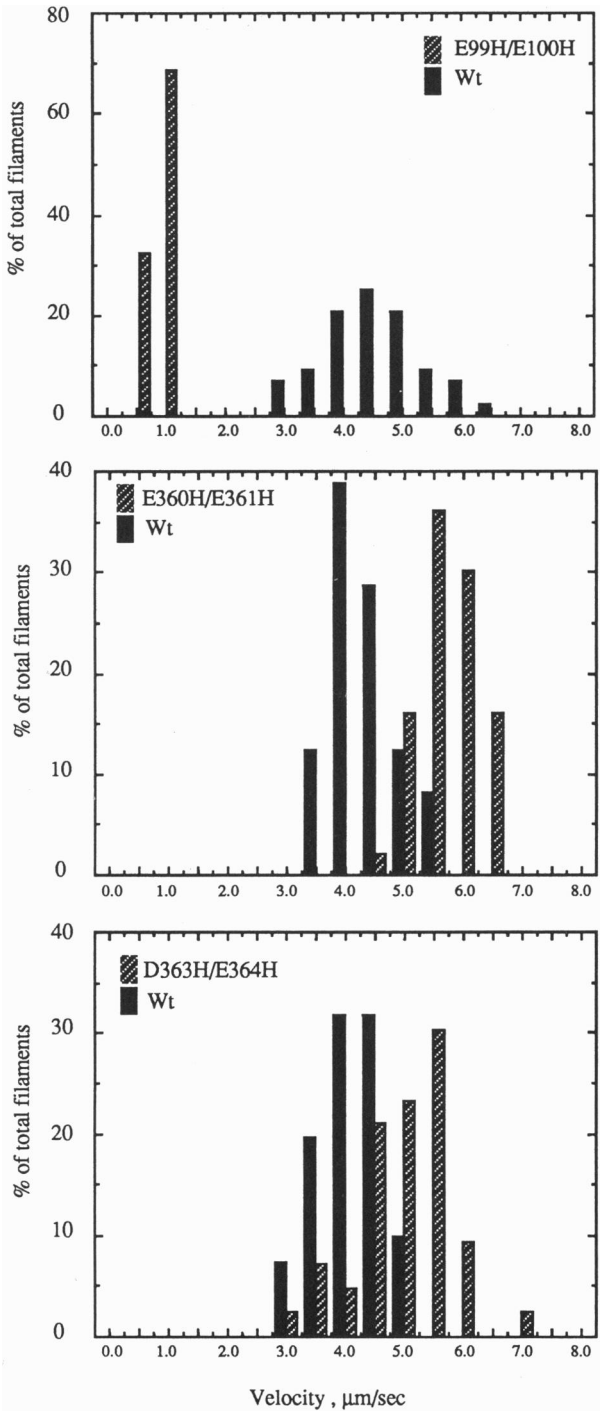

FIG. 2. Distribution of the sliding velocity of actin filaments. Measurements are carried out on nitrocellulose-coated glass at 25°C. Bars: solid, wild-type filaments (Wt); cross-hatched, mutant filaments. For E99H/E100H, only moving filaments (50% of total filaments at 25°C) were counted.

Force Measurements. Force generated by a single actin filament and myosin was measured by the glass needle method (28, 29). The average force generated by single E360H/E361H filaments was 8.1 ± 0.6 pN/μm of actin filament (n = 11). As a control, force measurements were carried out using single filaments of wild-type actin on the same batch of silicon-coated glass. The average force generated by the control actin was 9.6 ± 0.9 pN/μm (n = 11). Another set of measurements was carried out for D363H/E364H filaments. They generated 6.0 ± 0.2 pN/μm (n = 7). The control wild-type actin generated 7.7 ± 1.9 pN/μm (n = 4). The results summarized in Table 1 indicate that mutations at the C-terminal cluster of acidic residues did not significantly affect force generation.

Force measurements for E99H/E100H filaments were hampered by a small number of filament bundles in F-actin preparations that easily stuck to the glass needle.

Measurements of Actin-Activated ATPase Activity. A mutation at D24/D25 resulted in the complete loss of the activation of HMM ATPase activity, consistent with the loss of motility. Mutations at E360/E361 and at D363/E364 affected the activation to some extent. Actin-activated HMM ATPase activities (V) at various concentrations (S) of wild-type actin, E360H/E361H, and D363H/E364H are shown in Fig. 3 in S/V vs. S plots. Apparent affinities of actin and HMM in the presence of MgATP (K_m) and the turnover rates at infinite actin concentration (V_{max}) were estimated from the plot by the least squares method. K_m and V_{max} values thus obtained were 19 μM and 10 s^{-1} for wild-type actin and 47 μM and 12 s^{-1} for E360H/E361H. Mutations at E360/E361 increased the K_m, whereas the V_{max} remain unchanged. For D363H/E364H, the exact values of K_m and V_{max} could not be obtained since the ATPase activities increased almost linearly with increasing F-actin concentrations up to 70 μM. However, the rather large increase of both K_m and V_{max} values by the mutation is easily recognized in Fig. 3C.

Activation by E99H/E100H could not be assessed because of the tendency of filaments of this mutant actin to associate at higher concentrations. F-actin filaments could not be

Table 1. *In vitro* assays

Actin	Motility ratio		Force ratio
	NC	S	
Wild	1.00	1.00	1.00
D24H/D25H	Nonmotile	ND	ND
E99H/E100H	0.17 (0.8/4.8)	ND	ND
E360H/E361H	1.30 (6.0/4.6)	0.95 (6.5/6.8)	0.84 (8.1/9.6)
D363H/E364H	1.21 (5.2/4.3)	0.88 (4.4/5.0)	0.78 (6.0/7.7)

Ratio of sliding velocities (motilities) of mutant actin to wild-type actin on a nitrocellulose-coated (NC) or a silicon-coated (S) glass surface is shown. Sliding on the nitrocellulose-coated surface is driven by HMM; sliding on the silicon-coated surface is driven by full-length myosin. Actual average values of sliding velocity in μm/sec are in parentheses (velocity of mutant/velocity of wild type). Ratio of force generated by mutant actin to that by wild-type actin is shown. Force was generated by a single actin filament and full-length myosin molecules on a silicon-coated glass surface. Actual average values of force in pN/μm of filament are in parentheses (force by mutant/force by wild type). ND, not done.

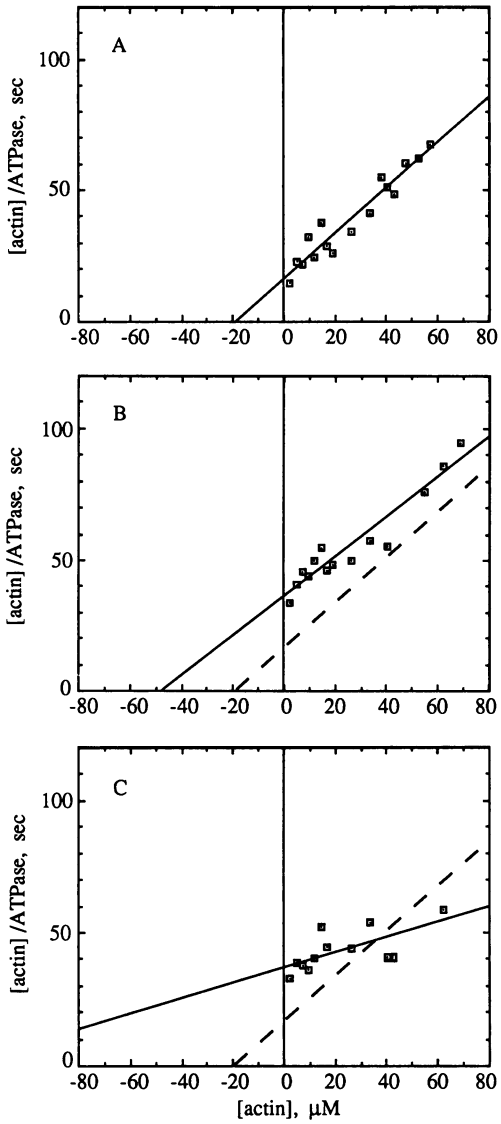

FIG. 3. Actin-activated HMM ATPase activity. S/V vs. S plot (V, ATPase activities; S, actin concentrations). (*A*) Wild-type actin. (*B*) E360H/E361H. (*C*) D363H/E364H. Dotted lines in *B* and *C* represent the best fit line for data in *A*.

dispersed to homogeneity once centrifuged to remove residual phosphate, a necessary step for our ATPase assays.

DISCUSSION

A mutation at D24/D25 resulted in the loss of motility with a concomitant loss of activation of HMM ATPase activity. However, the mutant was able to form the ATP-sensitive rigor complex with myosin, indicating that the observed loss of motility and activation of HMM ATPase activity resulted from a local change of charge distribution on actin, not from gross structural changes. In this context, it must be noted that D24/D25 are on a loop exposed on the surface of actin (1) that may adapt to an amino acid replacement without disruptive structural changes. Thus, we conclude that D24/D25 are essential for ATP-driven sliding and, possibly, force generation.

Mutations at E99/E100 located on another loop (1) also affected the sliding of F-actin. E99H/E100H behaved like the D1H/D4H mutant we have described (12). Their sliding motion was not continuous. They moved for a while, stopped, and then resumed sliding. Velocity of E99H/E100H filament sliding was only 17% of that of wild-type F-actin, whereas the velocity of sliding D1H/D4H filaments was reduced to 20%. These results indicate that residues E99 and E100 are involved in ATP-driven sliding as are the N-terminal acidic residues.

The C-terminal cluster of acidic residues E360/E361/D363/E364 is one of the most densely charged surface areas on actin. Three of the acidic residues (E361/D363/E364) are highly conserved among actins. In the absence of MgATP, the area is actually in contact with the N-terminal segment of the alkaline light chain 1 of myosin (3, 5). A mutation at D363/E364 resulted in a rather large increase of both K_m and V_{max} values. A mutation at E360/E361 resulted in an increase of K_m whereas V_{max} was unchanged. Thus, both mutations changed kinetic steps of the ATPase cycle to some extent. However, these mutations only slightly affected sliding and force generation. It must be noted that the relationship of the overall kinetics of ATP hydrolysis to sliding and to force generation is not straightforward (31, 32), since these processes may be limited by different kinetic steps of the actin-activated ATP hydrolysis cycle. It is likely that mutations at the C-terminal cluster of acidic residues, especially at D363/E364, affected a kinetic step(s) that was not directly coupled to sliding or force generation.

In summary, our mutational mappings showed that the N terminus, D24/D25, and E99/E100 of actin are involved in myosin-driven sliding and, possibly, force generation. The C-terminal cluster of acidic residues E360/E361/D363/E364 is not essential for sliding and force generation, though some of these residues may be involved in a kinetic step(s) of the ATP hydrolysis cycle not directly coupled to these processes.

This work was supported by a Grant-in-Aid for Specially Promoted Research (02102009) from the Ministry of Education, Science and Culture of Japan.

1. Kabsch, W., Mannhertz, H. G., Suck, D., Pai, E. F. & Holmes, K. C. (1990) *Nature (London)* **347**, 37–44.
2. Holmes, K. C., Popp, D., Gebhard, W. & Kabsch, W. (1990) *Nature (London)* **347**, 44–49.
3. Milligan, R. A., Whittaker, M. & Safer, D. (1990) *Nature (London)* **348**, 217–221.
4. Holmes, K. C., Tirion, M., Popp, D., Lorenz, M., Kabsch, W. & Milligan, R. A. (1992) in *Mechanism of Miofilament Sliding in Muscle Contraction*, eds. Sugi, H. & Pollack, G. H. (Plenum, New York).
5. Sutoh, K. (1983) *Biochemistry* **22**, 1579–1585.
6. Mejean, C., Boyer, M., Labbe, P. J., Marlier, L., Benyamin, Y. & Roustan, C. (1987) *Biochem. J.* **244**, 571–577.
7. Miller, L., Kalnoski, M., Yunossi, Z., Bulinski, J. C. & Reisler, E. (1987) *Biochemistry* **26**, 6064–6070.
8. Bertrand, R., Chaussepied, P. & Kassab, R. (1988) *Biochemistry* **27**, 5728–5736.
9. DasGupta, G. & Reisler, E. (1989) *J. Mol. Biol.* **207**, 833–836.
10. Labbe, J. P., Mejean, C., Benyamin, Y. & Roustan, C. (1990) *Biochem. J.* **271**, 407–411.
11. DasGupta, G. & Reisler, E. (1992) *Biochemistry* **31**, 1836–1841.
12. Sutoh, K., Ando, M., Sutoh, K. & Yano-Toyoshima, Y. (1991) *Proc. Natl. Acad. Sci. USA* **88**, 7711–7714.
13. Aspenstrom, P. & Karlsson, R. (1991) *Eur. J. Biochem.* **200**, 35–41.
14. Cook, R. K., Blake, W. T. & Rubenstein, P. A. (1992) *J. Biol. Chem.* **267**, 9430–9436.
15. Aspenstrom, P., Lindberg, U. & Karlsson, R. (1992) *FEBS Lett.* **303**, 59–63.
16. Kron, S. J. & Spudich, J. A. (1986) *Proc. Natl. Acad. Sci. USA* **83**, 6272–6276.
17. Harada, Y., Noguchi, A., Kishino, A. & Yanagida, T. (1987) *Nature (London)* **326**, 805–808.
18. Kunkel, T. A. (1985) *Proc. Natl. Acad. Sci. USA* **82**, 488–492.
19. Knecht, D., Cohen, S. M., Loomis, W. F. & Lodish, H. F. (1986) *Mol. Cell. Biol.* **6**, 3973–3983.
20. Early, A. E. & Williams, J. G. (1987) *Gene* **59**, 99–106.
21. Sambrook, J., Fritsch, E. F. & Maniatis, T. (1989) *Molecular Cloning: A Laboratory Manual* (Cold Spring Harbor Lab., Cold Spring Harbor, NY), 2nd Ed.

22. Nellen, W., Datta, S., Reymond, C., Sivertsn, A., Mann, S., Crowley, T. & Firtel, R. A. (1987) *Methods Cell Biol.* **28,** 67–100.
23. Howard, P. K., Ahern, K. G. & Firtel, R. A. (1988) *Nucleic Acids Res.* **16,** 2613–2623.
24. O'Farrell, P. M. (1975) *J. Biol. Chem.* **250,** 4007–4021.
25. Weeds, A. G. & Taylor, R. S. (1975) *Nature (London)* **257,** 54–56.
26. Yano-Toyoshima, Y., Kron, S. J., McNally, E. M., Niebling, K. R., Toyoshima, C. & Spudich, J. A. (1987) *Nature (London)* **328,** 536–539.
27. Harada, Y., Sakurada, K., Aoki, T., Thomas, D. D. & Yanagida, T. (1990) *J. Mol. Biol.* **216,** 49–68.
28. Kishino, A. & Yanagida, T. (1988) *Nature (London)* **334,** 74–76.
29. Ishijima, A., Doi, T., Sakurada, K. & Yanagida, T. (1991) *Nature (London)* **352,** 301–306.
30. Kodama, T., Fukui, K. & Kometani, K. (1986) *J. Biochem. (Tokyo)* **99,** 1465–1472.
31. Prochniewicz, E. & Yanagida, T. (1990) *J. Mol. Biol.* **216,** 761–772.
32. Umemoto, S., Bengur, A. R. & Sellers, J. R. (1989) *J. Biol. Chem.* **264,** 1431–1436.